THE JOURNAL OF BIOLOGICAL CHEMISTRY VOL. 282, NO. 15, pp. 11436–11445, April 13, 2007
Printed in the U.S.A.

Conformation-sensitive Antibodies against Alzheimer Amyloid-β by Immunization with a Thioredoxin-constrained B-cell Epitope Peptide*

Received for publication, October 16, 2006, and in revised form, January 31, 2007 Published, JBC Papers in Press, January 31, 2007, DOI 10.1074/jbc.M609690200

Nadia Moretto[‡], Angelo Bolchi[‡], Claudio Rivetti[‡], Bruno P. Imbimbo[§], Gino Villetti[§], Vladimiro Pietrini[¶], Luciano Polonelli[‖], Steven Del Signore[‡‡], Karen M. Smith[**‡‡], Robert J. Ferrante[**‡‡], and Simone Ottonello[‡1]**

*From the [‡]Department of Biochemistry and Molecular Biology, [§]Chiesi Farmaceutici, R & D Department, [¶]Department of Neurosciences, Neurology Section, and [‖]Department of Pathology and Laboratory Medicine, University of Parma, 43100 Parma, Italy, **Geriatric Research Education and Clinical Center, Bedford Veterans Affairs Medical Center, Department of Veterans Affairs, Bedford, Massachusetts 01730, and [‡‡]Departments of Neurology, Pathology, and Psychiatry, Boston University School of Medicine, Boston, Massachusetts 02118*

Immunotherapy against the amyloid-β (Aβ) peptide is a valuable potential treatment for Alzheimer disease (AD). An ideal antigen should be soluble and nontoxic, avoid the C-terminally located T-cell epitope of Aβ, and yet be capable of eliciting antibodies that recognize Aβ fibrils and neurotoxic Aβ oligomers but not the physiological monomeric species of Aβ. We have described here the construction and immunological characterization of a recombinant antigen with these features obtained by tandem multimerization of the immunodominant B-cell epitope peptide Aβ1–15 (Aβ15) within the active site loop of bacterial thioredoxin (Trx). Chimeric Trx(Aβ15)$_n$ polypeptides bearing one, four, or eight copies of Aβ15 were constructed and injected into mice in combination with alum, an adjuvant approved for human use. All three polypeptides were found to be immunogenic, yet eliciting antibodies with distinct recognition specificities. The anti-Trx(Aβ15)$_4$ antibody, in particular, recognized Aβ42 fibrils and oligomers but not monomers and exhibited the same kind of conformational selectivity against transthyretin, an amyloidogenic protein unrelated in sequence to Aβ. We have also demonstrated that anti-Trx(Aβ15)$_4$, which binds to human AD plaques, markedly reduces Aβ pathology in transgenic AD mice. The data indicate that a conformational epitope shared by oligomers and fibrils can be mimicked by a thioredoxin-constrained Aβ fragment repeat and identify Trx(Aβ15)$_4$ as a promising new tool for AD immunotherapy.

Antipeptide antibodies are valuable tools for probing structure-function relationships in proteins as well as for therapeutic and diagnostic applications. When immunotherapy is the ultimate goal, the sequence span of the peptide, and thus the nature of the epitope(s) associated with it, as well as the conformational selectivity of the resulting antibodies may also be dictated by safety reasons. This is the case of the amyloid-β (Aβ)[2] peptide, a major neuropathological hallmark (1–3) and a promising immunotherapeutic target of Alzheimer disease (AD) (4–7). Following the encouraging results obtained with Aβ42 vaccination in transgenic mouse models of AD (8–10), a Phase II clinical trial utilizing preaggregated Aβ42 as an antigen and the QS-21 saponin as an immunoadjuvant (AN-1792 vaccine) was halted due to the occurrence of meningoencephalitis in ~6% of treated patients (11–13). T-cell-mediated autoimmunity produced by the C-terminal portion of Aβ (14) along with a predominantly pro-inflammatory (T helper 1) immunoresponse and cross-reactivity with the presumably physiological monomeric forms of Aβ (Aβ38–43 peptides plus the amyloid-β precursor protein have been hypothesized as the main causes of these adverse effects (15–17). Of further concern is the fact that not only plaques but also soluble Aβ oligomers should be bound by a therapeutically effective antibody (18–20). The latter represent an intermediate conformation prior to fibril formation and are presently considered as the most proximate causative agents of AD (21–24).

Some of the above limitations have been overcome through the development of alternative immunogens relying on N-terminally located B-cell epitope-bearing fragments rather than on full-length Aβ (25–33). Also important in this regard is the availability of Aβ peptide formulations capable of eliciting antibodies that recognize specific assembly states of Aβ42 (19, 34–36). For example, antibodies binding to oligomeric and fibrillar (but not to monomeric) Aβ, have been produced by using purified Aβ42 oligomers (19) or nitrated Aβ40 (35) as antigens, whereas antibodies selectively recognizing soluble Aβ oligomers have been obtained by immunization with Aβ40 immobilized onto gold nanoparticles (36). Interestingly, the latter antibodies bind not only to Aβ oligomers but also to the oligomeric forms of various Aβ-unrelated amyloidogenic polypeptides, suggesting that a common (as yet unidentified) conformation-dependent structure is shared by soluble oligomers regardless of their sequence (36).

* Work carried out in the laboratory of R. J. F. was supported by the NIA, National Institutes of Health Grant AG13846 and the Department of Veterans Affairs. The costs of publication of this article were defrayed in part by the payment of page charges. This article must therefore be hereby marked "*advertisement*" in accordance with 18 U.S.C. Section 1734 solely to indicate this fact.

[1] To whom correspondence should be addressed: Dept. of Biochemistry and Molecular Biology, Parco Area delle Scienze 23/A 43100 Parma, Italy. Tel.: 39-0521-905646; Fax: 39-0521-905151; E-mail: s.ottonello@unipr.it.

[2] The abbreviations used are: Aβ, amyloid-β; AD, Alzheimer disease; APP, amyloid-β precursor protein; ELISA, enzyme-linked immunosorbent assay; PBS, phosphate-buffered saline; Trx, bacterial thioredoxin; TTR, human transthyretin.

A similar conformational selectivity has not been achieved so far with a T-cell epitope lacking a fragment of Aβ. Despite the lack of detailed information on the molecular basis of the conformational mimics generated by chemical modification or surface immobilization of the Aβ peptide, it is clear that some kind of structural constraining is involved. We thus reasoned that a similar conformational effect, besides an enhanced peptide stabilization and immunogenicity (37, 38), might be obtained with the use of a scaffold protein, such as thioredoxin, with the ability to constrain the structure of short peptides inserted within its surface-exposed active site loop (38–40) and to stimulate T-cell proliferation (41, 42). This kind of recombinant antigen would be highly desirable because of its expected safety, ease of construction, and large scale production in a chemically homogeneous form.

We have shown here that antibodies recognizing Aβ42 oligomers and fibrils (but not monomers) are produced by immunization with a 4-fold repeat of the Aβ15 peptide bearing an interposed three-amino-acid linker and arranged in tandem within the display site of bacterial thioredoxin (Trx). As revealed by comparison with Trx(Aβ15)$_n$ antigens bearing one or eight copies of Aβ15, conformational selectivity critically depends on Aβ15 multiplicity and on the use of multipeptide insertions fitting the structural constraining capacity of Trx. We have further documented the ability of the anti-Trx(Aβ15)$_4$ antibody to bind Aβ aggregates in human brain and to ameliorate AD pathology in APP transgenic mice.

EXPERIMENTAL PROCEDURES

TrxAβ Constructs—Chimeric Trx polypeptides bearing the Aβ15 or the Aβ42 peptide (TrxAβ) were constructed by using a modified pET28 plasmid (Novagen), designated as pT7Kan-Trx, harboring the sequence for an N- and C-terminally His$_6$-tagged version of bacterial thioredoxin along with a kanamycin resistance marker. The unique CpoI site present within the Trx coding sequence (nucleotide positions 99–105, corresponding to amino acid residues 34–35) was used as the cloning site. The phosphorylated oligonucleotides 5′-gtccgatggatgcagaattccgacatgactcaggatatgaagttcatcatcaaggcg-3′ (forward) and 5′-gaccgccttgatgatgaacttcatatcctgagtcatgtcggaattctgcatccatcg-3′ (reverse), both bearing 5′-protruding CpoI sequences (underlined), were annealed and ligated to CpoI-digested pT7Kan-Trx at a 1:10 vector:insert molar ratio. The resulting construct, pT7Kan-TrxAβ15, encodes a polypeptide, Trx-(1–33)gPMDAEFRHDSGYEVHHQGGpTrx (36–109) in which Aβ15 (underlined) is preceded by a Met residue at the N terminus and is followed by the Gly-Gly-Pro linker at the C terminus (with the Gly and Pro residues provided by the inserted ds-oligonucleotide and by the Trx scaffold, respectively). Constructs bearing multiple copies of Aβ15 were generated in a similar way but at a 1:100 vector:insert molar ratio using the sequence-verified insert excised from pT7-Kan-TrxAβ15 as starting material. Recombinant clones were screened by restriction analysis, and two of them, bearing four or eight copies of Aβ15, were selected. Essentially identical experimental conditions were used to construct TrxAβ42, which was cloned in both pT7Kan-Trx as well as in a companion vector (pT7Amp-Trx) carrying an ampicillin rather than a kanamycin antibiotic resistance marker.

Expression and Purification of the TrxAβ Polypeptides—Expression was induced by adding 1 mM isopropyl-β-D-thiogalactopyranoside to *Escherichia coli* BL21Star (DE3) cells (Invitrogen) transformed with each of the above constructs and allowed to proceed for 2 h at 37 °C. A different *E. coli* strain (Origami-DE3; Novagen) and modified expression conditions (pT7Amp-Trx vector; 5 h at 30 °C) were used for TrxAβ42, which was otherwise completely insoluble. Following cell lysis, His$_6$-tagged TrxAβ polypeptides were bound to a metal affinity resin (Talon; Clontech), purified according to the manufacturer's instructions, and extensively dialyzed against phosphate-buffered saline (PBS). Protein concentration was determined with the Coomassie dye method (Bio-Rad) and by UV light absorbance. The composition and purity of individual polypeptide preparations was assessed by gel electrophoresis on 11% polyacrylamide-SDS gels.

Immunization Protocols—TrxAβ polypeptides (2 mg/ml in PBS) were filter-sterilized, and an aliquot of each (10 nmol) was mixed with 1 mg of alum (Sigma-Aldrich) in a final volume of 400 μl immediately before use. Aβ42 (Sigma-Aldrich) was dissolved in PBS (2 mg/ml) and aggregated overnight at 37 °C prior to immunization. Five randomly assorted groups of one-month-old male BALB/c mice (10 animals each) (Charles River Laboratories) were injected subcutaneously with the above antigens at days 1, 15, 30, and 60, as specified in the legend to Fig. 2*A*. The same treatment was applied to two negative control groups that were injected with PBS and with aggregated Aβ42, both without alum. Sera were collected two weeks after the last boost and randomly pooled in pairs. A standard immunization protocol (three doses of Trx(Aβ15)$_4$ antigen in Freund adjuvant administered to one animal over a period of two months) was used to generate rabbit anti-Trx(Aβ15)$_4$ antibodies (SeqLab).

Detection of Anti-Aβ42 Antibodies—Total anti-Aβ42 antibodies were detected by enzyme-linked immunosorbent assay (ELISA) at a fixed 1:200 dilution, using aggregated Aβ42 (0.5 μg/well) as the target antigen (43). Following incubation, washing, and the addition of horseradish peroxidase-conjugated anti-mouse immunoglobulins (1/5000; Sigma-Aldrich) and the chromogenic substrate *o*-phenylendiamine (Sigma-Aldrich), plates were read spectrophotometrically at 450 nm. Immunoglobulin isotype determination was conducted at a fixed 1:200 dilution using rat anti-mouse Ig subclass-specific, horseradish peroxidase-conjugated secondary antibodies (TechniPharm). ELISAs were conducted in triplicate on the five-paired sera from each group; only a subset of sera from the three top responders in Groups 3, 4, 6, and 7 (see Fig. 2*A*) was utilized for isotype determination. Comparisons between groups were conducted by one-way analysis of variance using Analyze-it software.

Immunohistochemistry—Sera from mice immunized with each of the three Trx(Aβ15)$_n$ polypeptides were screened for their ability to bind Aβ plaques in human brain sections from a 68-year-old patient with neuropathological and clinical symptoms typical of severe AD. Various dilutions (1:100–1:1000) of pooled sera from the three top responders in Groups 5, 6, and 7

were analyzed. Sera were added to serial 8-μm brain sections of formalin-fixed, temporal cortical tissue, pretreated with formic acid (80%, 15 min). Sera from mock-treated animals (PBS; Group 1) and a commercial anti-Aβ40 polyclonal antibody (Anti-Pan β-Amyloid, BIOSOURCE) were used as negative and positive controls, respectively. Immunolabeling was revealed with the EnVision Plus/horseradish peroxidase system (Dako), using 3–3′-diaminobenzidine as the chromogenic substrate, according to the manufacturer's instructions. Images were captured with a digital camera at magnifications ranging from 50 to 400×.

Immunodot Blot Assays and Atomic Force Microscopy Imaging—A stock solution of trifluoroacetic acid-pretreated, monomeric Aβ42 peptide (1 mM) was prepared as described previously (44) and diluted to the required Aβ42 final concentration (2–50 μM) with 0.1% trifluoroacetic acid prior to immunodot blot analysis. Aβ42 dissolved in 2 M dimethyl sulfoxide (1 mM final concentration) was utilized for the preparation of aggregated Aβ42 species (19, 21, 45). A 10-fold dilution of the above stock solution into cold Ham's F-12 K medium (phenol red-free; BIOSOURCE) followed by incubation at 4 °C for 24 h was used to produce soluble oligomers; the same stock solution diluted into 10 mM HCl at a final concentration of 100 μM and incubated for 24 h at 37 °C was used to generate Aβ fibrils. Aβ oligomer and fibril formation, as well as the absence of fibrillar aggregates in soluble oligomer preparations, were verified by atomic force microscopy. To this end, samples of the above-described Aβ42 preparations were diluted 10-fold in 20 μl of deposition buffer (4 mM HEPES, pH 7.4, 10 mM NaCl, 7 mM $MgCl_2$) and immediately deposited onto freshly cleaved ruby mica at room temperature. After 5 min, mica disks were rinsed with milli-Q grade water and gently dried under a stream of nitrogen. Images were collected with a Nanoscope III microscope (Digital Instruments) operated in tapping mode using commercial diving board silicon cantilevers (MikroMasch). Oligomer formation was also checked by electrophoretic analysis on Tris-Tricine polyacrylamide gels followed by silver staining as described in Ref. 19. Samples of recombinant $Ile^{84} \rightarrow Ser$ transthyretin (Ser^{84}-TTR) enriched in soluble oligomers or higher order fibrillar aggregates were prepared by incubating the protein (2 mg/ml) for either 2 or 96 h at 37 °C in 100 mM sodium-acetate buffer (pH 4.0) as described in Refs. 46 and 47; control samples of monomeric Ser^{84}-TTR were obtained from parallel incubations in 50 mM K-phosphate buffer (pH 7.6). For dot blot analysis, the various Aβ42 or Ser^{84}-TTR species were hand-spotted onto nitrocellulose membranes (GE Healthcare) pre-wetted with TBS (20 mM Tris-HCl, pH 7.5, 0.8% NaCl) (19). Antisera for dot blot analysis were affinity-purified on protein-A minicolumns (Diatheva) according to the manufacturer's instructions. Following the determination of total immunoglobulin concentration with the Coomassie dye method, purified immunoglobulins were used for dot blot assays at a final concentration of 0.75 μg/ml. After blocking at room temperature with 5% nonfat dry milk in TBS supplemented with 0.05% Tween 20 (TBST), the blots were incubated for 1.5 h with each of the three anti-Trx$(Aβ15)_n$ antibodies in dry milk-TBST, washed 3 × 10 min with TBST, followed by mouse immunoglobulin detection with the SuperSignal West Femto kit (Pierce), as specified by the manufacturer. To distinguish between monomer and oligomer binding, affinity-purified anti-monomeric TrxAβ15 antibodies (0.75 μg/ml) were preincubated (2 h at 4 °C under stirring conditions) with a 50-fold molar excess of the monomeric Aβ42 peptide in TBS prior to hybridization. At least two replicates were carried out for each of the 15 pools of antisera from the various Trx$(Aβ15)_n$-treated groups (see Fig. 2*A*, *Groups 5–7*). Dot blot images were quantified with the Quantity One program (Bio-Rad). Signal volume intensities for individual Aβ42 species within each membrane were averaged, and the resulting data were plotted with Sigma Plot (SPSS).

Surgery and Neuropathological Evaluation of Transgenic AD Mice—Female transgenic AD (Tg2576) mice expressing the Swedish mutation of human APP (48) were obtained from the Boston University Alzheimer Disease Center mouse colony. Founders for this colony were provided by Dr. Karen Hsiao-Ashe (Department of Neurology, University of Minnesota Medical School). The APP Tg2576 mice developed behavioral abnormalities and exhibited histological evidence of brain Aβ deposits as plaques along with associated astrogliosis from as early as 8 months. Mice were genotyped using a standardized PCR assay on tail DNA and were housed four in each cage under standard conditions with *ad libitum* access to food and water. Six 14-month-old APP mice (32–34 g each), placed on a 12-h light schedule, were used for surgeries. Mice were anesthetized with ketamine HCl/xylazine intraperitoneal injection (100 mg/kg ketamine and 10 mg/kg xylazine; 100 μl/10 g body weight) and were positioned in a stereotaxic apparatus (Koph) with a mouse head adaptor. Thermoregulation was maintained at 37 °C using a warming pad with respiratory monitoring throughout the procedure. The scalp was incised in the midline to expose the sagittal suture, and stereotaxic coordinates in both hemispheres were determined (49). The bregma was used as a reference point (−2.0 mm), and holes were drilled in the calvarium at the junction of the left and right lateral coordinates (1.75 mm). Affinity-purified anti-Trx$(Aβ15)_4$ antibodies along with mock immunoglobulins from PBS-treated mice (2 μl each) were stereotaxically injected into the left and right hippocampi (−2.0 mm ventral), respectively, using a blunt-tipped 10-μl syringe (Hamilton). Upon syringe placement, there was a 2-min dwell time followed by a 4-min injection time and an additional 2-min dwell time prior to removal of the syringe. A topical antiseptic was applied as the incision was closed using a 9-mm autoclip. Mice were kept on a warming pad until full recovery. All animal experiments were performed in accordance with the National Institutes of Health Guide for the Care and Use of Laboratory Animals and both the Department of Veterans Affairs and Boston University Animal Care committees. Seven days post-injection, the mice were deeply anesthetized and transcardially perfused with 2% buffered paraformaldehyde (100 ml). Brains were post-fixed for 2 h, cryoprotected in a graded series of glycerol, and subsequently frozen-sectioned (50 μm). Serially cut mouse tissue sections were stained for Nissl substance, immunostained with anti-Aβ42 (catalog number 344; BIOSOURCE International), anti-Aβ oligomer (A11; BIOSOURCE International), and glial fibrillary antigen protein (Dako) antibodies and silver-stained

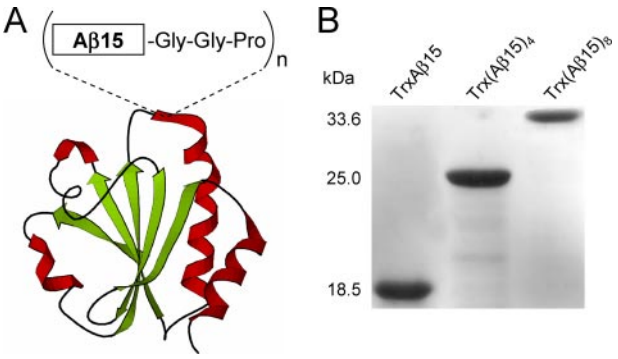

FIGURE 1. **Construction of Trx(Aβ15)$_n$ chimeras.** *A*, schematic representation of Trx-displayed Aβ15 peptides with their associated tripeptide linker. *B*, SDS-PAGE analysis of the purified Trx(Aβ15)$_n$ polypeptides.

using the Campbell-Switzer method for identification of mature Aβ plaques. Immunostained coronal tissue sections, serially cut within the hippocampus beginning from interaural (1.68 mm)/bregma (−2.12 mm) to interaural (2.16 mm)/bregma (−1.64 mm), were analyzed. Aβ-positive plaques were quantified from high resolution images of the same brain areas within the anti-Trx(Aβ15)$_4$-treated hemisphere and the contralateral mock-treated hemisphere using BioVision (50) and Neurolucida software programs (MicroBrightField, Williston, VT). BioVision differentiates and counts plaques from the background neuropil, whereas Neurolucida extracts the data from the BioVision images, exporting it to Excel (Microsoft, Redmond, WA) for statistical analysis.

RESULTS

Design and Construction of the Trx(Aβ15)$_n$ Polypeptides—The choice of Aβ15 as a peptide epitope was based on the lack of T-cell reactivity and good solubility previously ascribed to N-terminal peptides encompassing the first 15 residues of Aβ (4, 14, 27, 30, 43, 51). Trx was chosen because of its small size (109 amino acids) and solubility, structural rigidity, ability to act as a nontoxic immunoenhancer capable of stimulating murine T-cell proliferation, and presence of a convenient restriction site (CpoI) within its solvent-accessible active site loop (40–42). Insertions into this loop are usually well tolerated, and grafting both ends of the inserted peptide provides a conformational constraint that are neither achievable with N- or C-terminal fusions nor with random chemical cross-linking of peptides to a protein carrier (38–40). To mimic different assembly states of Aβ and to overcome the poor immunogenicity of short Aβ fragments (25, 27), Trx(Aβ15)$_n$ polypeptides bearing a single copy or multiple tandemly arranged copies of Aβ15 were constructed. A cloning strategy relying on the use of an excess of the Aβ15 DNA insert with respect to a modified recipient vector bearing the Trx coding sequence under the control of a phage T7 promoter (see "Experimental Procedures") was utilized for Trx(Aβ15)$_n$ construction (Fig. 1*A*). Constructs bearing one, four, or eight copies of Aβ15 were used to express the corresponding polypeptides, which were then purified by metal affinity chromatography (Fig. 1*B*). Instrumental to the production of properly assembled Aβ15 multimers were the directionality and in-frame fusion capability of the unique CpoI site present within the Trx active site loop region as well as the incorporation into Aβ15 DNA of a terminal sequence coding for an intervening Gly-Gly-Pro linker, thus also preventing the formation of junctional epitopes (52). A fourth construct (TrxAβ42) bearing a single copy of the full-length Aβ42 peptide was prepared in a similar way (see "Experimental Procedures" for details). Although all Trx(Aβ15)$_n$ polypeptides were completely soluble, regardless of Aβ15 multiplicity, most of the TrxAβ42 protein ended up in inclusion bodies in an insoluble form (not shown). Thus, Aβ42 appears to be poorly soluble, even when fused to Trx in the heterologous context of bacterial cells.

Immunological Characterization of the Trx(Aβ15)$_n$ Polypeptides—Five groups of 10 male BALB/c mice were treated with 10 nmol of the above-described Trx(Aβ15)$_n$ polypeptides or with equivalent amounts of preaggregated synthetic Aβ42 or TrxAβ42, all supplemented with alum, an immunoadjuvant approved for human use (Fig. 2*A*). Two additional groups injected with buffer alone (PBS) or with alum-free Aβ42 served as negative controls. No adverse side effect was observed in animals injected with four doses of the various Trx(Aβ15)$_n$ polypeptides over a period of two months. Sera were collected two weeks after the fourth injection and randomly pooled in pairs, and the five resulting pools were analyzed with ELISA using aggregated fibrillar Aβ42 as the target antigen. As shown in Fig. 2*A*, mean anti-Aβ antibody levels elicited by Trx(Aβ15)$_4$ and Trx(Aβ15)$_8$ (but not monomeric TrxAβ15) were significantly higher ($p \leq 0.05$) than those of mock-treated controls and similar to those of the Aβ42-treated groups, where TrxAβ42 performed as well as free Aβ42. An anti-inflammatory T helper 2-polarized response, typical of the alum adjuvant (14, 25, 53), was revealed by isotype profiling (Fig. 2*B*). Although a prevalence of IgG1 was observed with all antigens, the IgG1:IgG2a ratio, an indicator of T helper 2 polarization, was reproducibly higher ($p \leq 0.05$) for multimeric Trx(Aβ15)$_n$ and TrxAβ42 immunoconjugates than for unconjugated Aβ42.

Detection of Aβ Aggregates in Human Brain by Anti-Trx(Aβ15)$_n$ Antibodies—The ability of antisera generated in response to Trx(Aβ15)$_n$ to bind amyloid plaques was investigated next. This property, which is considered the best prognostic indication of *in vivo* anti-Aβ antibody efficacy (26), is not shared by all previously described anti-Aβ antibodies (*e.g.* m266 and other antibodies targeting the C-terminal portion of Aβ42 (26)). As shown in Fig. 3, sera from mice immunized with the tetrameric (Fig. 3*A*) or the octameric (Fig. 3*B*) form of Trx(Aβ15)$_n$ bound to amyloid plaques up to a dilution of 1:1000. Large neuritic plaques, as well as mature and immature plaques, were labeled by anti-multimeric Trx(Aβ15)$_n$ antibodies. A broader immunostaining, especially within senile plaque cores, was observed with the positive control anti-Pan β-amyloid antiserum generated in rabbits using Aβ40 as the antigen (not shown). By comparison, no plaques were detected either with sera from mock-treated animals (not shown) or with sera from mice immunized with monomeric TrxAβ15 (Fig. 3*C*).

Differential Recognition of Distinct Aβ Assembly States by Anti-Trx(Aβ15)$_n$ Antibodies—Immunodot blot assays were used then to assess the recognition selectivity of the various anti-Trx(Aβ15)$_n$ antibodies toward different assembly states of

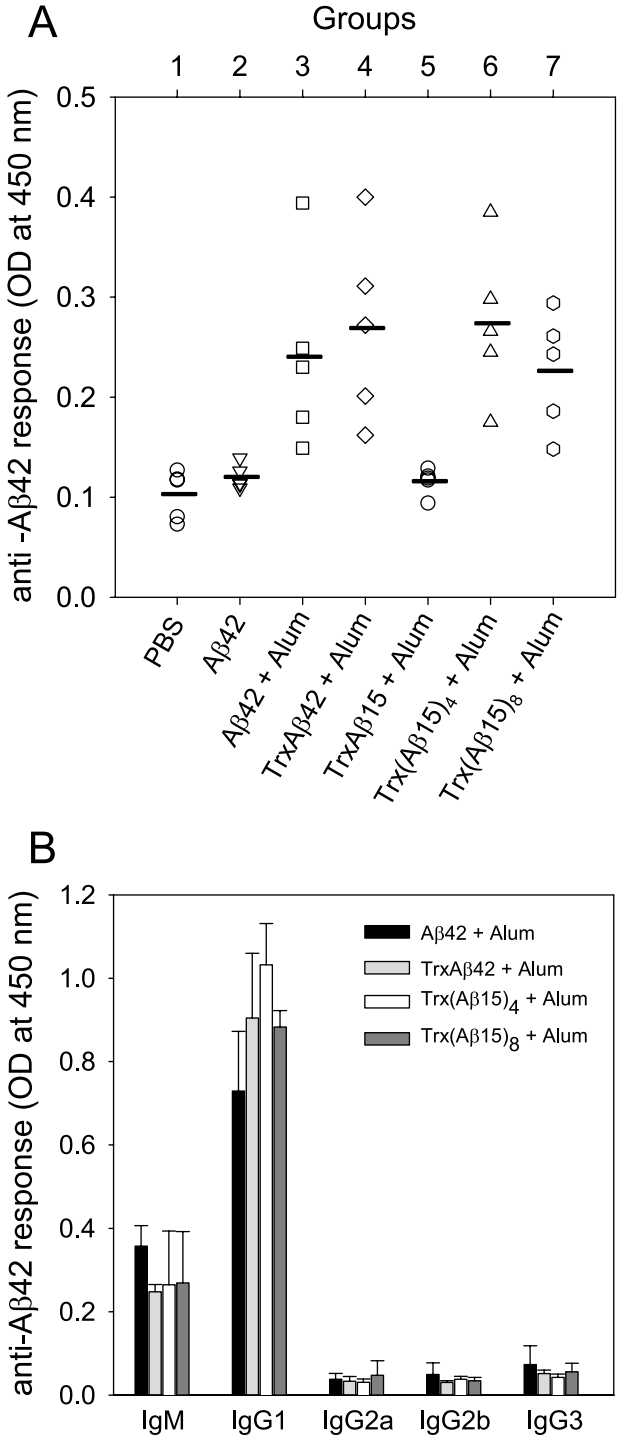

FIGURE 2. **Immunological characterization of Trx(Aβ15)$_n$ polypeptides.** *A*, anti-Aβ42 reactivity of sera from mice immunized with the indicated Trx(Aβ15)$_n$ polypeptides (*Groups 5–7*), with preaggregated synthetic Aβ42 (*Group 3*), or TrxAβ42 (*Group 4*), all adjuvanted with alum, or mock-immunized with either adjuvant-free Aβ42 (*Group 2*) or PBS (*Group 1*) (see "Experimental Procedures" for details). ELISA data for five randomly paired pools of sera from each group were obtained using aggregated synthetic Aβ42 as target antigen and are presented as a scatter plot; the Aβ binding activity of the 35 individual pools as well as the mean binding activity of each of the seven groups (*bars*) are shown. *B*, immunoglobulin isotypes of antisera from the three top responders in each immunopositive group (*3*, *4*, *6*, and *7*).

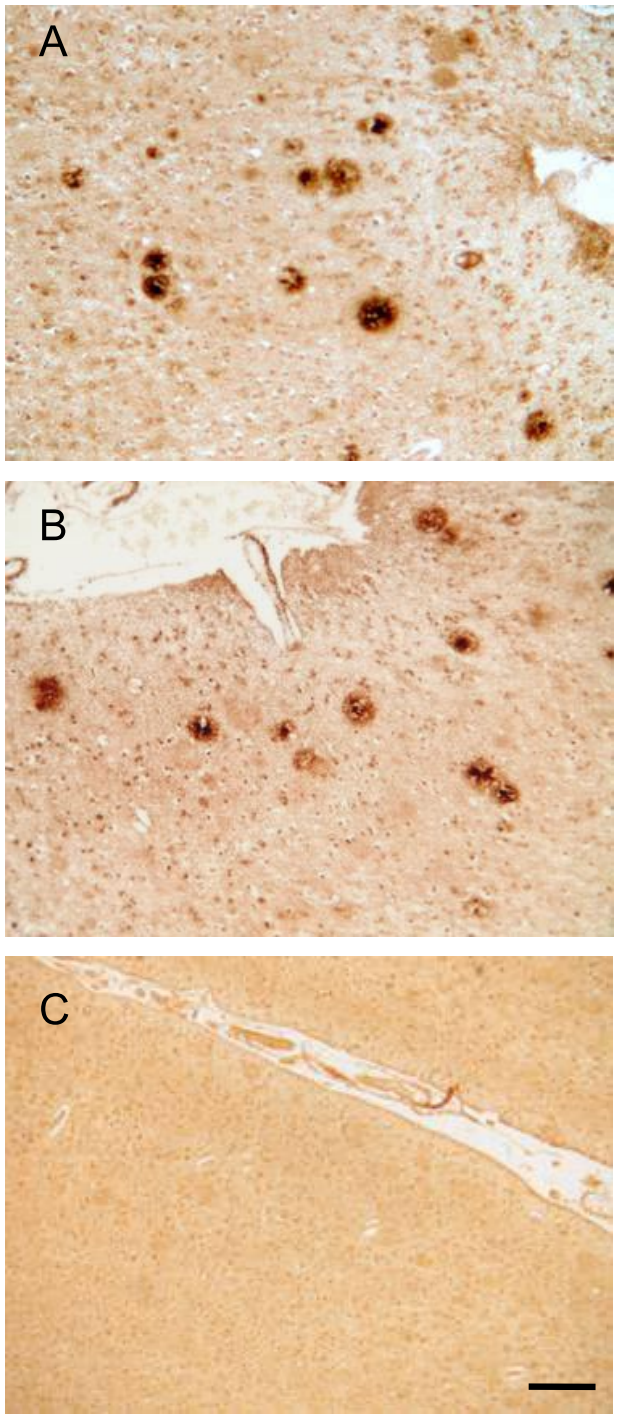

FIGURE 3. **Antibodies produced by immunization with tetrameric and octameric (but not monomeric) Trx(Aβ15)$_n$, bind to amyloid plaques (*dark brown spots*) in the brain.** Temporal cortex sections from a patient with severe AD were treated with sera from mice immunized with Trx(Aβ15)$_4$ (*A*), Trx(Aβ15)$_8$ (*B*), or TrxAβ15 (*C*). *Scale bar*, 100 μm.

Aβ42 (monomers, oligomers, and fibrils) generated *in vitro* under previously determined conditions (21, 45). Fibril formation, the lack of Aβ aggregates in the monomer solution, as well as the lack of fibrils in the oligomer preparation were verified by atomic force microscopy (Fig. 4*A*). Silver-stained polyacrylamide gels were used to evaluate oligomer preparations, which in keeping with previous reports (19, 21, 45) and despite prolonged incubation in F-12 medium, were found to contain ~50% residual monomer, with trimers and tetramers as the most represented oligomeric species (Fig. 4*B*). As shown in Fig. 4*C*, antibodies from mice immunized with monomeric

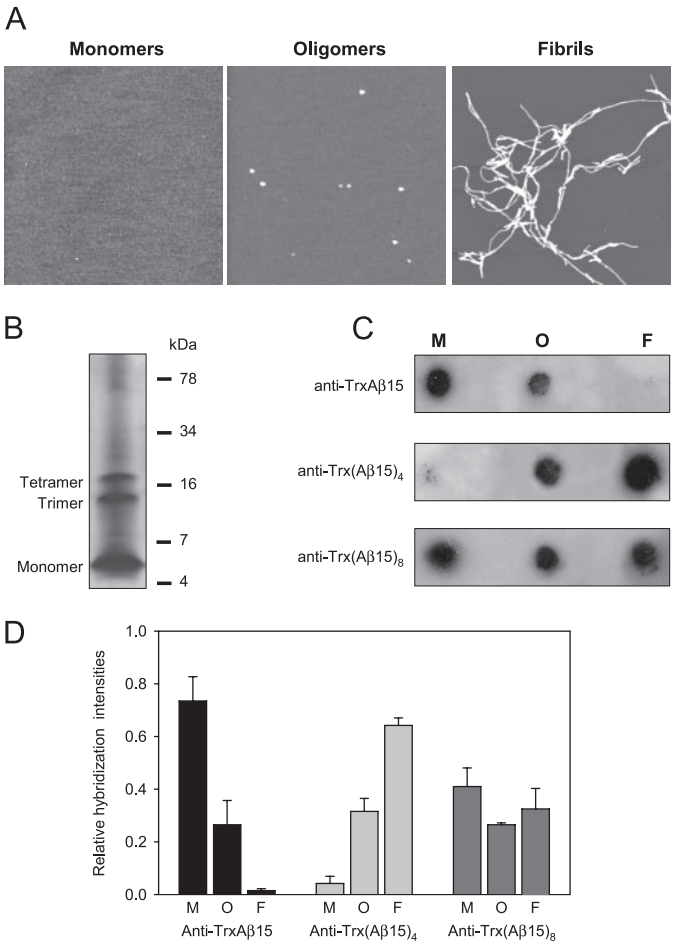

FIGURE 4. **Differential recognition of distinct Aβ assembly states by antibodies raised against different Trx(Aβ15)$_n$ polypeptides.** *A*, representative 2 × 2 μm atomic force microscopy images of the indicated Aβ42 species; total *z*-ranges (*left to right*) are 2, 12, and 13 nm. *B*, silver-stained SDS-PAGE of a typical Aβ42 oligomer preparation; the migration positions of individual Aβ42 species and of molecular mass markers are indicated. *C*, representative results obtained from immunodot blot assays carried out at a fixed concentration (0.75 μg/ml) of the indicated affinity-purified anti-Trx(Aβ15)$_n$ antibodies and 10 pmol of the various Aβ42 species (*M*, monomers; *O*, oligomers; *F*, fibrils). *D*, differential recognition profiles of antibodies from the five pools of antisera in each of the Trx(Aβ15)$_n$-treated groups (Group 5, anti-Trx(Aβ15); Group 6, anti-Trx(Aβ15)$_4$; Group 7, anti-Trx(Aβ15)$_8$; see Fig. 2*A*). Dot blot assays (at least two replicates for each pool) were conducted as described for *C* and quantified; signal volume intensities for individual Aβ42 species within each membrane were averaged. Cumulative data for the three groups are expressed as relative values (± S.D.) for each Aβ42 species, normalized with respect to the sum of the average hybridization signal intensities measured for all Aβ42 species.

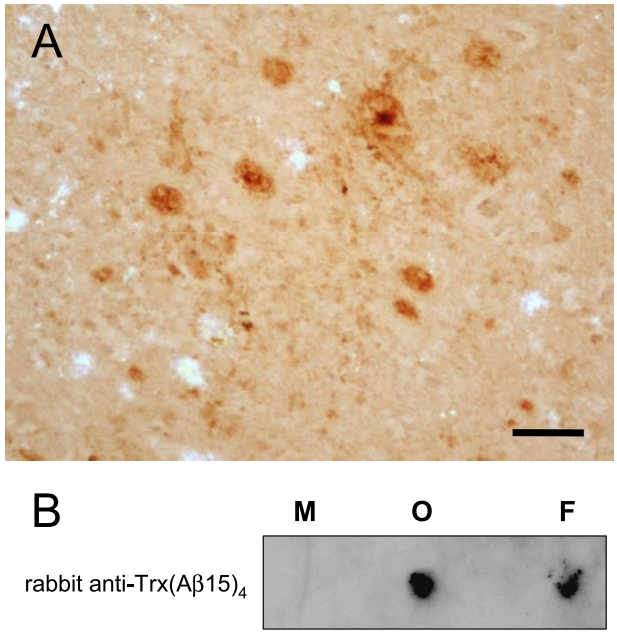

FIGURE 5. **Aβ recognition properties of a rabbit anti-Trx(Aβ15)$_4$ antiserum obtained with Freund's adjuvant.** *A*, immunostaining of amyloid plaques (*dark brown spots*) in human brain. *Scale bar*, 100 μm. *B*, immunodot blot assay of different Aβ42 species (*M*, monomers; *O*, oligomers; *F*, fibrils (10 pmol each)).

TrxAβ15 do not bind to Aβ fibrils, in accordance with their inability to recognize higher order Aβ42 aggregates in ELISAs or Aβ fibrils in AD plaques (see Figs. 2*A* and 3*C*), yet they appear to react with both monomers and oligomers. However, because of the presence of sizeable amounts of monomeric Aβ in the oligomer preparation (see Fig. 4*B*), it is likely that Aβ monomers, rather than oligomers, are the actual targets of anti-monomeric TrxAβ15 antibodies. In fact, a loss of immunoreactivity was observed upon preincubation of these antibodies with an excess of the monomeric Aβ42 peptide (not shown). A different recognition pattern was observed with antibodies raised against Trx(Aβ15)$_4$, which recognized Aβ42 oligomers and fibrils but not monomers (Fig. 4*C*). In contrast but similar to the results obtained with the commercial 4G8 monoclonal antibody (not shown), all three Aβ42 species were bound by antibodies raised against Trx(Aβ15)$_8$ (Fig. 4*C*), thus indicating that excessive multimerization of the Aβ15 peptide leads to a loss of conformational selectivity. This also appears to be the case for a recently developed DNA immunogen composed of an unscaffolded 11-fold repeat of Aβ1–6 without an intervening spacer, which yielded antibodies that indiscriminately recognized monomeric and oligomeric Aβ42 species yet barely bound to higher order fibrillar aggregates (28). Importantly, as shown in Fig. 4*D*, the same differential recognition profile was shared by the different, randomly assorted pools of antisera raised against monomeric, tetrameric and octameric TrxAβ15. As further shown in Fig. 5, the same conformational selectivity along with the capacity to recognize human Aβ plaques were observed with a rabbit antiserum generated using Freund-adjuvanted Trx(Aβ15)$_4$ as antigen, thus suggesting that this property is neither influenced by the animal host nor the type of adjuvant utilized for immunization.

Additional evidence as to the conformational selectivity of anti-Trx(Aβ15)$_4$ antibodies was provided by an immunodot blot experiment testing their ability to recognize different assembly states of an amyloidogenic polypeptide unrelated in sequence to Aβ42. The Ile^{84} → Ser variant of human transthyretin, a strongly amyloidogenic protein (54), was used for this purpose. As shown in Fig. 6, although with a reduced immunoreactivity, the same differential recognition pattern observed with Aβ42 (*i.e.* the binding of higher order fibrillar aggregates and oligomers but not monomers) was observed with anti-Trx(Aβ15)$_4$ antibodies when challenged with different assembly states of Ser^{84}-TTR. As expected, no reactivity toward aggregated Ser^{84}-TTR was observed under the same conditions with antibodies raised against monomeric TrxAβ15 (not

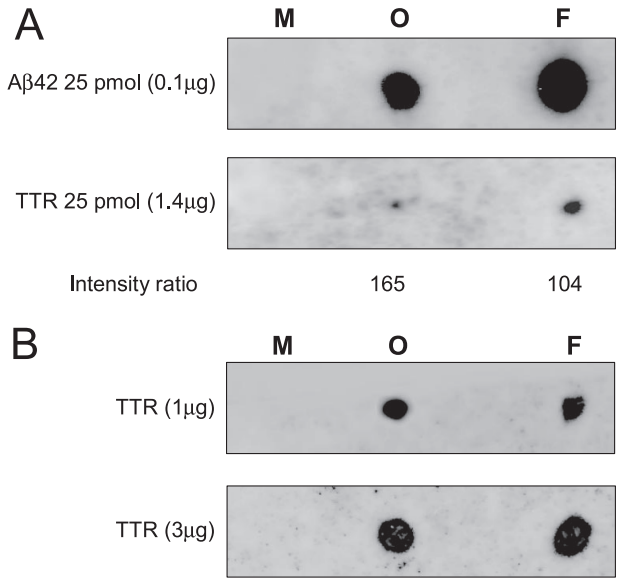

FIGURE 6. **Binding of anti-Trx(Aβ15)$_4$ antibodies to aggregated (but not monomeric) Ser^{84}-TTR.** *A*, affinity-purified anti-Trx(Aβ15)$_4$ antibodies (0.75 μg/ml) were comparatively analyzed for their ability to recognize distinct assembly states of Aβ42 and Ser^{84}-TTR (*M*, monomers; *O*, oligomers; *F*, fibrillar aggregates). The ratios between hybridization values for Aβ42 and Ser^{84}-TTR, obtained by densitometric analysis after 1 min of signal development, are shown *below* the *O* and *F rows*. *B*, binding of oligomeric and fibrillar Ser^{84}-TTR by anti-Trx(Aβ15)$_4$ antibodies visualized in an immunodot blot experiment carried out as described for *A* but with a longer signal development time (15 min).

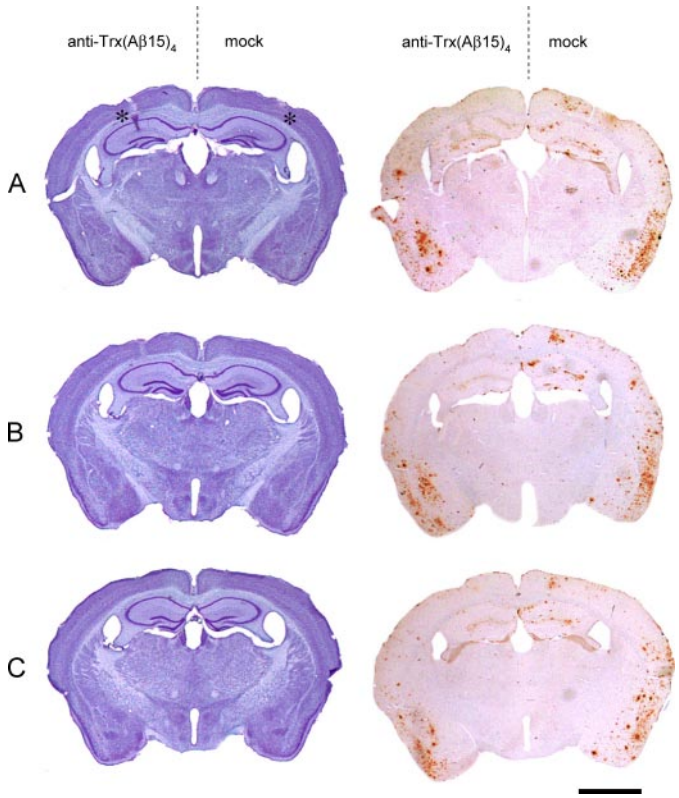

FIGURE 7. **Gross identification of stereotaxic injection sites in the APP Tg2576 mice.** Serially cut Nissl-stained sections and matching contiguous Aβ42-immunostained sections are shown on the *left* and *right* sides, respectively. Affinity-purified anti-Trx(Aβ15)$_4$ antibodies, along with mock immunoglobulins from PBS-treated mice (2 μl each), were stereotaxically injected into the left and right hippocampus as indicated; needle tracts are marked by *asterisks*. Tissue sections, 1 and 2 mm rostral to the injection sites, are shown in *B* and *C*, respectively. Adjacent immunostained sections in *A–C* show a marked reduction of Aβ42-positive plaques close to the anti-Trx(Aβ15)$_4$ injection site and penumbra. *Scale bar*, 2 mm.

shown), thus further strengthening the notion that these antibodies selectively recognize Aβ monomers.

Anti-Trx(Aβ15)$_4$ Antibody Clears Aβ Pathology in APP Transgenic AD Mice—The immunotherapeutic potential of anti-Trx(Aβ15)$_4$ was evaluated next by stereotaxically injecting this antibody into the hippocampus of 14-month-old APP transgenic AD (Tg2576) mice. Mock immunoglobulins injected into the contralateral hemisphere from mice treated with PBS only served as an internal control for this experiment. Seven days post-injection, histopathological examination and plaque quantitation revealed a significant ($p < 0.01$) reduction of Aβ immunostaining in the anti-Trx(Aβ15)$_4$-injected hemispheres ($0.97 \times 10^3 \pm 0.27$ plaques) compared with the mock-injected hemispheres ($3.34 \times 10^3 \pm 0.58$ plaques) (Figs. 7 and 8, *A–C*). Aβ-positive plaques were not only absent at the injection site but significantly diminished within the injection penumbra (2 mm anterior/posterior to the injection site) (Figs. 7 and 8, *A–C*). As shown in Fig. 8*D*, similar results were obtained with an antibody that selectively reacts with soluble high molecular weight Aβ40 and Aβ42 oligomers (36). This indicates that the clearing effect of anti-Trx(Aβ15)$_4$ does not depend on the particular primary antibody utilized for immunodetection and suggests that also higher order oligomers (23) are targeted *in vivo* by the anti-Trx(Aβ15)$_4$ antibody. To verify that these findings were not the result of a competition between anti-Trx(Aβ15)$_4$ and the primary anti-Aβ antibody, we performed alternative histopathological analyses using glial fibrillary antigen protein immunostaining and Campbell-Switzer silver staining to detect astrogliosis and Aβ plaques. An amyloid plaque-associated astroglial response, increasing with the severity of disease progression, has been reported in APP mice (55). As shown in Fig. 9, *A* and *B*, astrogliosis and glia-associated plaques were markedly reduced within the anti-Trx(Aβ15)$_4$ antibody injection penumbra compared with the contralateral mock-injected hemisphere. In addition, as revealed by Campbell-Switzer silver staining, there were far fewer plaques in the anti-Trx(Aβ15)$_4$-injected hemisphere compared with the mock-injected hemisphere (*cf.* the *left* and the *right panels* in Fig. 9*C*). Both observations are consistent with the immunostaining data obtained with anti-Aβ antibody detection.

DISCUSSION

As revealed by this study, Trx(Aβ15)$_4$ is a soluble derivative of Aβ with good immunogenicity even when formulated with a moderate strength adjuvant, such as alum, that promotes an anti-inflammatory T helper 2-polarized immunoresponse. Even more significant, Trx(Aβ15)$_4$ is the first B-cell epitope Aβ antigen that is shown to be capable of generating antibodies that bind to Aβ fibrils and synaptotoxic Aβ oligomers but not to the presumably physiological monomeric species of Aβ. In this regard, anti-Trx(Aβ15)$_4$ antibodies resemble assembly state selective antibodies previously developed by using preassembled Aβ42 oligomers (19) or the nitrated Aβ40 peptide (35) as antigens. The main difference here is that a selected Aβ fragment, rather than full-length Aβ, was used as a recombinant

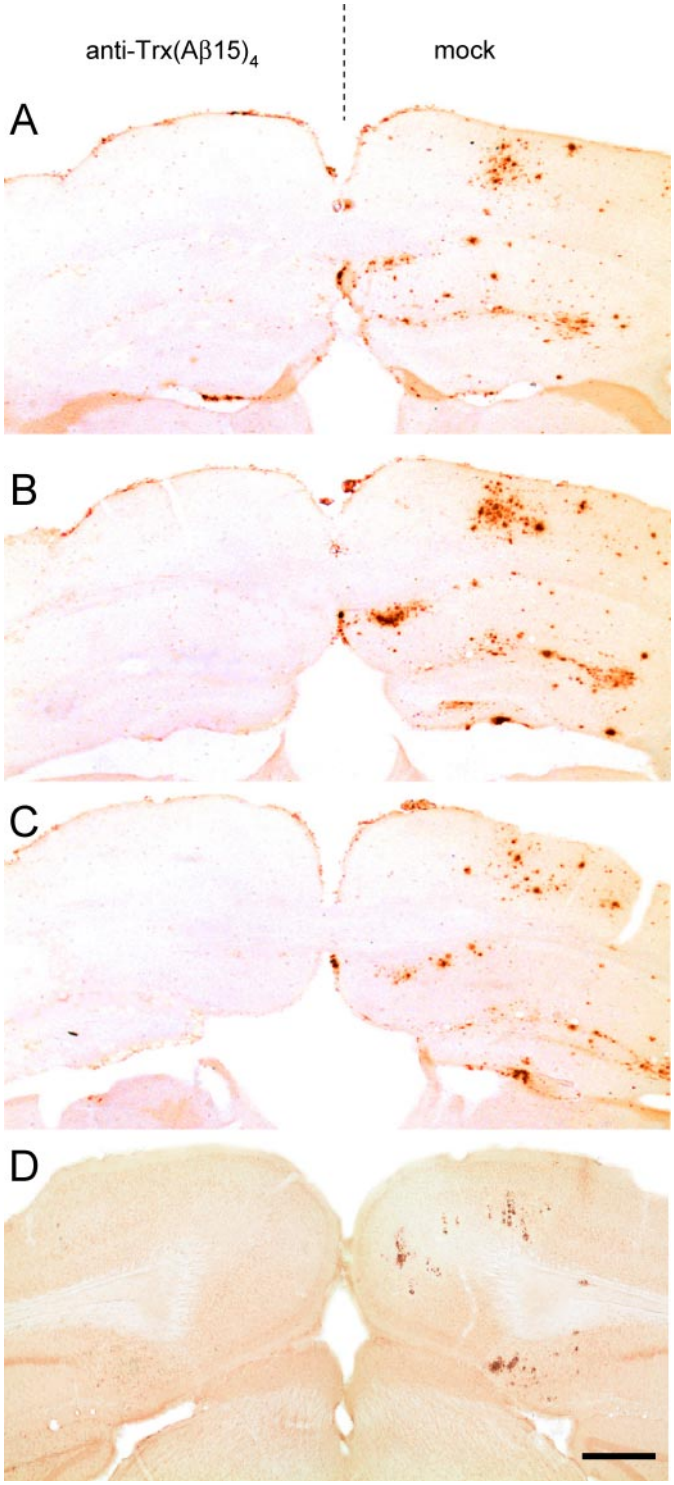

FIGURE 8. **Clearance of Aβ pathology by anti-Trx(Aβ15)$_4$ viewed at a higher magnification and with a different primary antibody.** High power view of brain sections from Tg2576 mice stereotaxically injected as described in the legend to Fig. 7 (anti-Trx(Aβ15)$_4$, left hemisphere; mock, right hemisphere), immunostained with either a universal anti-Aβ42 antibody (*A–C*) or an anti-oligomer-selective antibody (*D*) (see "Experimental Procedures" for details). Sections corresponding to the injection site or to the penumbra, shown in *A* and in *B–D*, respectively, evidence the lack of Aβ-positive plaques in the hippocampus and overlying cortex of the anti-Trx(Aβ15)$_4$-injected hemisphere. *Scale bar*, 500 μm.

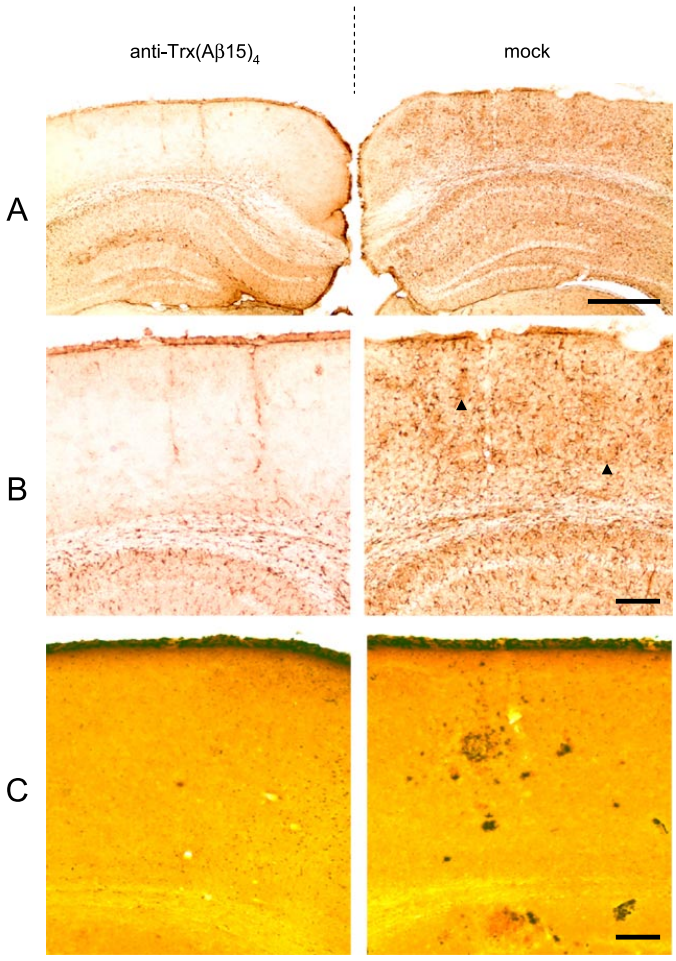

FIGURE 9. **Anti-Trx(Aβ15)$_4$ treatment reduces astrogliosis as well as the number of silver-positive plaque structures.** Tissue sections from stereotaxically injected Tg2576 mice (anti-Trx(Aβ15)$_4$, *left side*; mock, *right side*) were either immunostained with an antibody against glial fibrillary antigen protein, a histological marker of astrogliosis (*panels A* and *B*), or silver-stained with the Campbell-Switzer method (*C*). At low (*A*; *scale bar*, 500 μm) and high (*B*; *scale bar*, 100 μm) magnification, glial fibrillary antigen protein immunostaining reveals little or no reactive astrogliosis and glia-associated plaques (*arrowheads* in *B*) in the anti-Trx(Aβ15)$_4$-injected side (*left*) in contrast to the mock-injected side (*right*). A similar effect of the anti-Trx(Aβ15)$_4$ antibody on plaque burden, detected with Campbell-Switzer silver staining, is shown in *C*.

antigen and that antibodies with differential recognition properties were generated simply by varying the copy number of the Aβ15 peptide within the display site of thioredoxin. The ability of anti-Trx(Aβ15)$_4$ antibodies to recognize oligomeric and fibrillar aggregates of a different amyloidogenic protein such as TTR, is reminiscent of the "pan-amyloid reactivity" previously observed with antibodies raised against sonicated Aβ40 fibrils (34) or Aβ40 immobilized on gold nanoparticles (36) as structurally constrained antigens. Various hypotheses have been proposed to explain this cross-reactivity. For example, regardless of their amino acid sequence, all amyloids may share a cross-β pattern structure or other common features, such as a unique array of H-bond donors and acceptors (34). Apart from the, as yet, largely unknown structural determinants of this cross-reactivity, what our data suggest is that, when grafted to the active site loop of thioredoxin, the (Aβ15)$_4$ polypeptide is constrained into a conformation that mimics a structural epitope shared by both fibrils and neurotoxic soluble oligomers but not Aβ monomers. Conformational selectivity, coupled with enhanced immunogenicity, may increase the safety and efficacy of anti-Trx(Aβ15)$_4$ as an Aβ aggregate scavenger. This

expectation is supported by the immunotherapeutic performance of the anti-Trx(Aβ15)$_4$ antibodies, revealed by the *in vivo* experiments in APP transgenic AD (Tg2576) mice. These mice recapitulate many aspects of human AD and provide a means to investigate the temporal and spatial progression of several important neuropathological events, such as amyloid deposition and astrogliosis. Our experimental studies show significant amelioration of the neuropathological phenotype displayed by this AD mouse model following administration of the anti-Trx(Aβ15)$_4$ antibody.

Because of the above-mentioned favorable features, Trx(Aβ15)$_4$ lends itself as a prototype B-cell epitope vaccine for AD. Because of its recombinant nature and chemically defined molecular composition, Trx(Aβ15)$_4$ is also a promising candidate for a DNA vaccination approach for the production of monoclonal antibodies for passive immunization purposes as well as for structural analysis of its amyloid-like epitope.

Acknowledgments—We thank Fabrizio Tagliavini ("C. Besta" National Institute of Neurology and Department of Clinical Neurosciences, Milano, Italy) for human AD brain specimens, Mary Lambert (Department of Neurobiology and Physiology, Northwestern University) for a sample of anti-Aβ42 oligomer antiserum and for technical advice on immunodot blot assays, Claudia Folli and Rodolfo Berni (Department of Biochemistry and Molecular Biology, University of Parma) for the gift of recombinant Ser^{84}-TTR, and the Ann McKee laboratory (Boston University, School of Medicine) for help with the Campbell-Switzer method. The assistance of Stefania Conti, Lara Ravanetti, and Simona Arseni (Department of Pathology and Laboratory Medicine) with ELISA, Sara Cellai (Department of Biochemistry and Molecular Biology) with atomic force microscopy, and Maria Francesca Baroc (Department of Neurosciences) with human AD brain immunohistochemistry is also gratefully acknowledged. The central instrumentation facility of the University of Parma provided access to the atomic force microscope.

REFERENCES

1. McLean, C. A., Cherny, R. A., Fraser, F. W., Fuller, S. J., Smith, M. J., Beyreuther, K., Bush, A. I., and Masters, C. L. (1999) *Ann. Neurol.* **46,** 860–866
2. Lambert, M. P., Barlow, A. K., Chromy, B. A., Edwards, C., Freed, R., Liosatos, M., Morgan, T. E., Rozovsky, I., Trommer, B., Viola, K. L., Wals, P., Zhang, C., Finch, C. E., Krafft, G. A., and Klein, W. L. (1998) *Proc. Natl. Acad. Sci. U. S. A.* **95,** 6448–6453
3. Selkoe, D. J. (2001) *Physiol. Rev.* **81,** 741–766
4. McLaurin, J., Cecal, R., Kierstead, M. E., Tian, X., Phinney, A. L., Manea, M., French, J. E., Lambermon, M. H., Darabie, A. A., Brown, M. E., Janus, C., Chishti, M. A., Horne, P., Westaway, D., Fraser, P. E., Mount, H. T., Przybylski, M., and St. George-Hyslop, P. (2002) *Nat. Med.* **8,** 1263–1269
5. Monsonego, A., and Weiner, H. L. (2003) *Science* **302,** 834–838
6. Schenk, D., Hagen, M., and Seubert, P. (2004) *Curr. Opin. Immunol.* **16,** 599–606
7. Gelinas, D. S., DaSilva, K., Fenili, D., St. George-Hyslop, P., and McLaurin, J. (2004) *Proc. Natl. Acad. Sci. U. S. A.* **101,** 14657–14662
8. Schenk, D., Barbour, R., Dunn, W., Gordon, G., Grajeda, H., Guido, T., Hu, K., Huang, J., Johnson-Wood, K., Khan, K., Kholodenko, D., Lee, M., Liao, Z., Lieberburg, I., Motter, R., Mutter, L., Soriano, F., Shopp, G., Vasquez, N., Vandevert, C., Walker, S., Wogulis, M., Yednock, T., Games, D., and Seubert, P. (1999) *Nature* **400,** 173–177
9. Morgan, D., Diamond, D. M., Gottschall, P. E., Ugen, K. E., Dickey, C., Hardy, J., Duff, K., Jantzen, P., DiCarlo, G., Wilcock, D., Connor, K., Hatcher, J., Hope, C., Gordon, M., and Arendash, G. W. (2000) *Nature* **408,** 982–985
10. Janus, C., Pearson, J., McLaurin, J., Mathews, P. M., Jiang, Y., Schmidt, S. D., Chishti, M. A., Horne, P., Heslin, D., French, J., Mount, H. T., Nixon, R. A., Mercken, M., Bergeron, C., Fraser, P. E., St. George-Hyslop, P., and Westaway, D. (2000) *Nature* **408,** 979–982
11. Imbimbo, B. P. (2002) *Ann. Neurol.* **51,** 794
12. Orgogozo, J. M., Gilman, S., Dartigues, J. F., Laurent, B., Puel, M., Kirby, L. C., Jouanny, P., Dubois, B., Eisner, L., Flitman, S., Michel, B. F., Boada, M., Frank, A., and Hock, C. (2003) *Neurology* **61,** 46–54
13. Nicoll, J. A., Wilkinson, D., Holmes, C., Steart, P., Markham, H., and Weller, R. O. (2003) *Nat. Med.* **9,** 448–452
14. Cribbs, D. H., Ghochikyan, A., Vasilevko, V., Tran, M., Petrushina, I., Sadzikava, N., Babikyan, D., Kesslak, P., Kieber-Emmons, T., Cotman, C. W., and Agadjanyan, M. G. (2003) *Int. Immunol.* **15,** 505–514
15. Boche, D., Nicoll, J. A., and Weller, R. O. (2005) *Curr. Opin. Neurol.* **18,** 720–725
16. Hock, C., Konietzko, U., Streffer, J. R., Tracy, J., Signorell, A., Muller-Tillmanns, B., Lemke, U., Henke, K., Moritz, E., Garcia, E., Wollmer, M. A., Umbricht, D., de Quervain, D. J., Hofmann, M., Maddalena, A., Papassotiropoulos, A., and Nitsch, R. M. (2003) *Neuron* **38,** 547–554
17. Robinson, S. R., Bishop, G. M., and Munch, G. (2003) *BioEssays* **25,** 283–288
18. Klein, W. L., Krafft, G. A., and Finch, C. E. (2001) *Trends Neurosci.* **24,** 219–224
19. Lambert, M. P., Viola, K. L., Chromy, B. A., Chang, L., Morgan, T. E., Yu, J., Venton, D. L., Krafft, G. A., Finch, C. E., and Klein, W. L. (2001) *J. Neurochem.* **79,** 595–605
20. Klyubin, I., Walsh, D. M., Lemere, C. A., Cullen, W. K., Shankar, G. M., Betts, V., Spooner, E. T., Jiang, L., Anwyl, R., Selkoe, D. J., and Rowan, M. J. (2005) *Nat. Med.* **11,** 556–561
21. Chromy, B. A., Nowak, R. J., Lambert, M. P., Viola, K. L., Chang, L., Velasco, P. T., Jones, B. W., Fernandez, S. J., Lacor, P. N., Horowitz, P., Finch, C. E., Krafft, G. A., and Klein, W. L. (2003) *Biochemistry* **42,** 12749–12760
22. Gong, Y., Chang, L., Viola, K. L., Lacor, P. N., Lambert, M. P., Finch, C. E., Krafft, G. A., and Klein, W. L. (2003) *Proc. Natl. Acad. Sci. U. S. A.* **100,** 10417–10422
23. Lesné, S., Koh, M. T., Kotilinek, L., Kayed, R., Glabe, C. G., Yang, A., Gallagher, M., and Ashe, K. H. (2006) *Nature* **440,** 352–357
24. Walsh, D. M., Klyubin, I., Fadeeva, J. V., Cullen, W. K., Anwyl, R., Wolfe, M. S., Rowan, M. J., and Selkoe, D. J. (2002) *Nature* **416,** 535–539
25. Agadjanyan, M. G., Ghochikyan, A., Petrushina, I., Vasilevko, V., Movsesyan, N., Mkrtichyan, M., Saing, T., and Cribbs, D. H. (2005) *J. Immunol.* **174,** 1580–1586
26. Bard, F., Barbour, R., Cannon, C., Carretto, R., Fox, M., Games, D., Guido, T., Hoenow, K., Hu, K., Johnson-Wood, K., Khan, K., Kholodenko, D., Lee, C., Lee, M., Motter, R., Nguyen, M., Reed, A., Schenk, D., Tang, P., Vasquez, N., Seubert, P., and Yednock, T. (2003) *Proc. Natl. Acad. Sci. U. S. A.* **100,** 2023–2028
27. Leverone, J. F., Spooner, E. T., Lehman, H. K., Clements, J. D., and Lemere, C. A. (2003) *Vaccine* **21,** 2197–2206
28. Kim, H. D., Maxwell, J. A., Kong, F. K., Tang, D. C., and Fukuchi, K. (2005) *Biochem. Biophys. Res. Commun.* **336,** 84–92
29. Maier, M., Seabrook, T. J., Lazo, N. D., Jiang, L., Das, P., Janus, C., and Lemere, C. A. (2006) *J. Neurosci.* **26,** 4717–4728
30. Sigurdsson, E. M., Scholtzova, H., Mehta, P. D., Frangione, B., and Wisniewski, T. (2001) *Am. J. Pathol.* **159,** 439–447
31. Solomon, B. (2004) *Curr. Alzheimer Res.* **1,** 149–163
32. Zurbriggen, R., Amacker, M., Kammer, A. R., Westerfeld, N., Borghgraef, P., Van Leuven, F., Van der Auwera, I., and Wera, S. (2005) *J. Mol. Neurosci.* **27,** 157–166
33. Zamora, E., Handisurya, A., Shafti-Keramat, S., Borchelt, D., Rudow, G., Conant, K., Cox, C., Troncoso, J. C., and Kirnbauer, R. (2006) *J. Immunol.* **177,** 2662–2670
34. O'Nuallain, B., and Wetzel, R. (2002) *Proc. Natl. Acad. Sci. U. S. A.* **99,** 1485–1490
35. Lee, E. B., Leng, L. Z., Zhang, B., Kwong, L., Trojanowski, J. Q., Abel, T.,

and Lee, V. M. (2006) *J. Biol. Chem.* **281,** 4292–4299
36. Kayed, R., Head, E., Thompson, J. L., McIntire, T. M., Milton, S. C., Cotman, C. W., and Glabe, C. G. (2003) *Science* **300,** 486–489
37. Thai, R., Moine, G., Desmadril, M., Servent, D., Tarride, J. L., Menez, A., and Leonetti, M. (2004) *J. Biol. Chem.* **279,** 50257–50266
38. Binz, H. K., Amstutz, P., and Pluckthun, A. (2005) *Nat. Biotechnol.* **23,** 1257–1268
39. Blum, J. H., Dove, S. L., Hochschild, A., and Mekalanos, J. J. (2000) *Proc. Natl. Acad. Sci. U. S. A.* **97,** 2241–2246
40. Colas, P., Cohen, B., Jessen, T., Grishina, I., McCoy, J., and Brent, R. (1996) *Nature* **380,** 548–550
41. Bertini, R., Howard, O. M., Dong, H. F., Oppenheim, J. J., Bizzarri, C., Sergi, R., Caselli, G., Pagliei, S., Romines, B., Wilshire, J. A., Mengozzi, M., Nakamura, H., Yodoi, J., Pekkari, K., Gurunath, R., Holmgren, A., Herzenberg, L. A., and Ghezzi, P. (1999) *J. Exp. Med.* **189,** 1783–1789
42. Blum, H., Rollinghoff, M., and Gessner, A. (1996) *Cytokine* **8,** 6–13
43. Spooner, E. T., Desai, R. V., Mori, C., Leverone, J. F., and Lemere, C. A. (2002) *Vaccine* **21,** 290–297
44. Zagorski, M. G., Yang, J., Shao, H., Ma, K., Zeng, H., and Hong, A. (1999) *Methods Enzymol.* **309,** 189–204
45. Stine, W. B., Jr., Dahlgren, K. N., Krafft, G. A., and LaDu, M. J. (2003) *J. Biol. Chem.* **278,** 11612–11622
46. Lindgren, M., Sorgjerd, K., and Hammarstrom, P. (2005) *Biophys. J.* **88,** 4200–4212
47. Bonifacio, M. J., Sakaki, Y., and Saraiva, M. J. (1996) *Biochim. Biophys. Acta* **1316,** 35–42
48. Hsiao, K., Chapman, P., Nilsen, S., Eckman, C., Harigaya, Y., Younkin, S., Yang, F., and Cole, G. (1996) *Science* **274,** 99–102
49. Franklin, K. B. J., and Paxinos, G. (1997) *The Mouse Brain in Stereotaxic Coordinates*, Academic Press, San Diego, CA
50. Chubb, C., Inagaki, Y., Sheu, P., Cummings, B., Wasserman, A., Head, E., and Cotman, C. (2006) *Neurobiol. Aging* **27,** 1462–1476
51. Town, T., Tan, J., Sansone, N., Obregon, D., Klein, T., and Mullan, M. (2001) *Neurosci. Lett.* **307,** 101–104
52. Livingston, B., Crimi, C., Newman, M., Higashimoto, Y., Appella, E., Sidney, J., and Sette, A. (2002) *J. Immunol.* **168,** 5499–5506
53. Ghochikyan, A., Mkrtichyan, M., Petrushina, I., Movsesyan, N., Karapetyan, A., Cribbs, D. H., and Agadjanyan, M. G. (2006) *Vaccine* **24,** 2275–2282
54. Dwulet, F. E., and Benson, M. D. (1986) *J. Clin. Investig.* **78,** 880–886
55. Irizarry, M. C., McNamara, M., Fedorchak, K., Hsiao, K., and Hyman, B. T. (1997) *J. Neuropathol. Exp. Neurol.* **56,** 965–973

Conformation-sensitive Antibodies against Alzheimer Amyloid-β by Immunization with a Thioredoxin-constrained B-cell Epitope Peptide

Nadia Moretto, Angelo Bolchi, Claudio Rivetti, Bruno P. Imbimbo, Gino Villetti, Vladimiro Pietrini, Luciano Polonelli, Steven Del Signore, Karen M. Smith, Robert J. Ferrante and Simone Ottonello

J. Biol. Chem. 2007, 282:11436-11445.
doi: 10.1074/jbc.M609690200 originally published online January 31, 2007
